Concrete subjected to combined mechanical and thermal loading: New experimental insight and micromechanical modeling

Thomas Ring[1], **Matthias Zeiml**[1,2], **and Roman Lackner**[3]

[1]*Institute for Mechanics of Materials and Structures (IMWS), Vienna University of Technology*
Karlsplatz 13/202, 1040 Vienna, Austria
e-mail: thomas.ring@tuwien.ac.at, matthias.zeiml@tuwien.ac.at

[2]*Fritsch, Chiari and Parnter ZT GmbH*
Diesterweggasse 3, 1140 Vienna, Austria
e-mail: zeiml@fcp.at

[3]*Material-Technology Innsbruck (MTI), University of Innsbruck*
Technikerstraße 13, 6020 Innsbruck, Austria
e-mail: roman.lackner@uibk.ac.at

Abstract

The realistic description of the behavior of concrete under high temperature and mechanical loading is of great importance, especially in terms of the safety assessment of concrete structures subjected to extreme events like tunnel fires. In order to capture the complex chemical and physical processes in heated concrete, a micromechanical model, taking the composite nature of concrete into account, is presented in this paper. Based on experimental results obtained from specimens subjected to combined thermo-mechanical loading, a two-scale model formulated within the framework of continuum micromechanic is developed, giving access to the elastic properties as a function of temperature and load level.

Keywords: Concrete, Strain behavior, Young's modulus, Poisson's ratio, Temperature loading, Experiment, Modeling

1. Introduction

Concrete under combined mechanical and thermal loading exhibits a certain path dependence explained by the dependence of physical processes on the actual stress state within the material (see Refs. [1, 9, 10]). As regards the elastic properties of heated concrete, experimental data are reported in the literature (see Ref. [8, 9]). Moreover, the decrease of elastic properties of concrete is also defined in national and international standards, like in the Eurocode 2-1-2 [3]. In the present work, a micromechanical model for the prediction of the change of elastic properties shall be developed, starting with the experimental characterization of the strain behavior and elastic properties (see Sec. 2). In Sec. 3, a two-scale model accounting for the different behavior of aggregates and cement paste for predicting the elastic properties of heated concrete is presented.

2. Experiments

2.1. Testing device

A radiant heated electric oven is used to apply the thermal loading (see Fig. 1). The cylindrical oven is built around the mechanical testing device, allowing, the conduction of tests under both thermal and mechanical loading. In the experiments reported in this paper, cylindrical concrete specimens with a diameter of 100 mm and a height of 200 mm are tested. The aggregates of the considered concrete mixture (see Ref. [4]) mainly consists of silicia materials 89% (68% quartz and 21% feldspar). In order to monitor the deformations of the heated specimen, steel rings are mounted with steel bars transferring the deformation of the specimen to the outside of the heated oven (axial direction). In the radial direction, the steel bars, giving access to the radial deformation, directly point from the specimen to the outside of the oven.

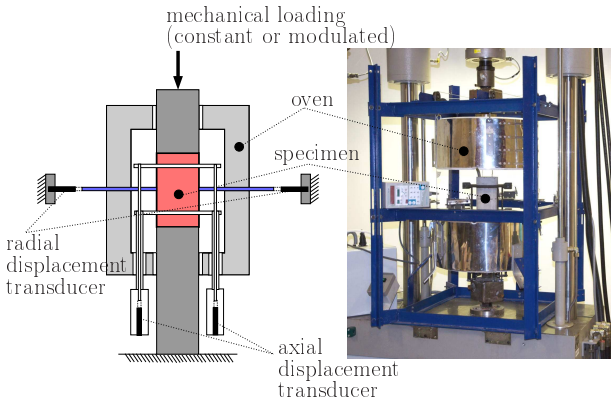

Figure 1: Used device for testing of heated concrete

2.2. Experimental results

In order to provide the basis for the sophisticated description of the combined mechanical and thermal behavior of concrete, the specimens are subjected to uniaxial loading and heated up to 800 °C with a heating rate of 1 °C/min. During the experiment, the radial and axial deformation of the specimens are monitored, with Figs. 2 and 3 showing the strain history in the axial (loaded) and radial (not loaded) direction.

The mechanical loading (load level s = 0, 10, 20, 30, 40, 50, 60% of $f_{c,0}$ (as the compressive strength at ambient temperature)) is applied before the temperature is increased and kept constant till the end of the experiment. The change in defor-

mation between 550 and 620 °C results from the quartz transition at 573 °C. The axial strain presented in Fig. 2 decreases with increasing loading. At higher load levels ($s \geq 40\%$), the specimen fails before the final temperature of 800 °C is reached. As regards the corresponding radial strain component, shown in Fig. 3, a continuous increase in strain is observed, which is more pronounced in case of higher mechanical loading.

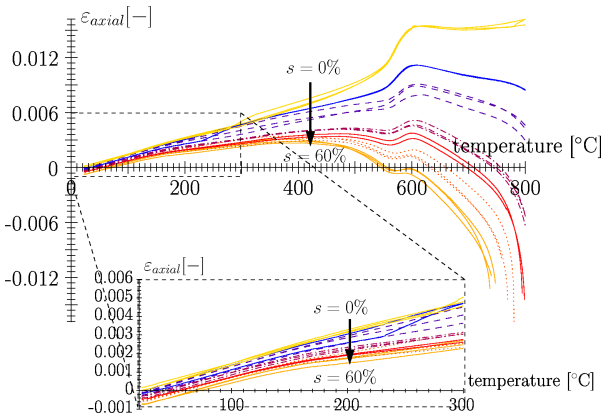

Figure 2: Axial-strain history under combined thermal (up to 800 °C) and mechanical loading (0-60% of initial compressive strength, with $f_{c,0} = 39.1$ MPa)

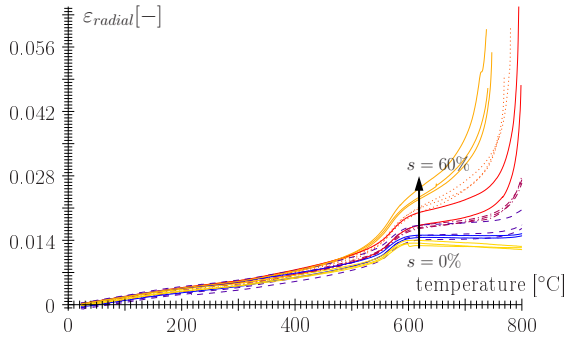

Figure 3: Radial-strain history under combined thermal (up to 800 °C) and mechanical loading (0-60% of initial compressive strength, with $f_{c,0} = 39.1$ MPa)

In order to identify the elastic properties of heated concrete, a modulated mechanical and steadily increasing thermal loading was considered within the test program. Hereby, mechanical loading oscillates around a prescribed load level (eg. $s = 10\%$ of $f_{c,0}$) with an amplitude of 16 kN and a period of 15 to 60 sec (see Fig. 4).

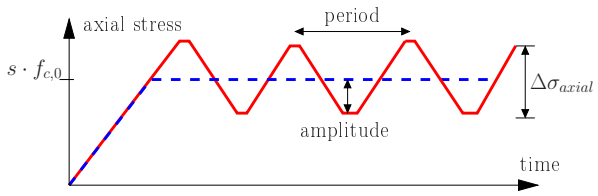

Figure 4: History of axial stress in modulated mechanical testing

Based on the displacements in axial as well as in radial direction, the actual Young's modulus and Poisson's ratio is determined as:

$$E(T,s) = \frac{\Delta\sigma_{axial}}{\Delta\varepsilon_{axial}} \tag{1}$$

and

$$\nu(T,s) = -\frac{\Delta\varepsilon_{radial}}{\Delta\varepsilon_{axial}}. \tag{2}$$

The evolution of Young's modulus and Poisson's ratio for one exemplary load level ($s = 20\%$) is presented in Figs. 5 and 6 and compared to the Young's modulus and Poisson's ratio of quartz (see Ref. [5]). The behavior of Young's modulus presented in Fig. 5 highlights the significant influence of the siliceous aggregates in the concrete mix. The temperature of quartz inversion at 573 °C shows a minimum in the evolution of Young's modulus. From that temperature till 700 °C the inversion on quartz leads to a slight increase of stiffness of the specimen.

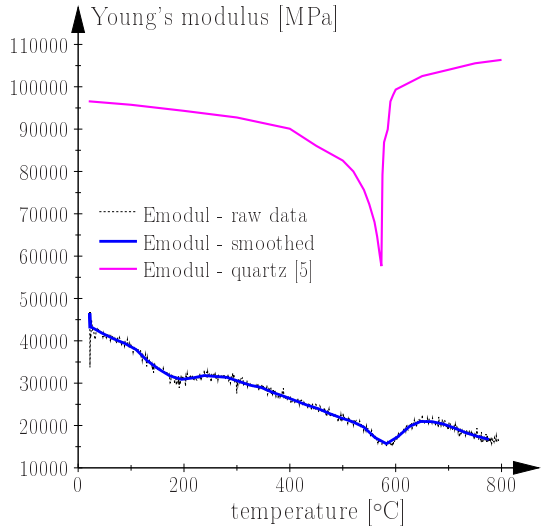

Figure 5: Young's modulus obtained from a combined modulated mechanical ($s = 20\%$) and steadily increasing thermal loading compared to Young's modulus of quartz [5]

The evolution of Poisson's ratio (see Fig. 6) is not smooth, which is explained by the deformation in radial direction being close to the accuracy of the measurement device. Similar to Young's modulus, the evolution of Poisson's ratio is driven by the behavior of the aggregates. At the temperature of quartz inversion at 573 °C, Poisson's ratio becomes negative. For temperatures above 573 °C, Poisson's ratio is increasing up to 0.4 at 800 °C.

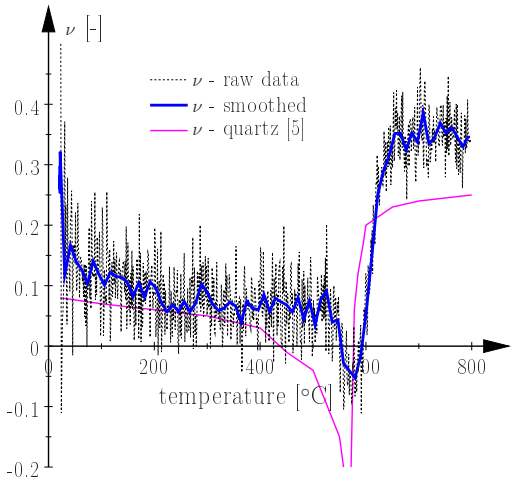

Figure 6: Poisson's ratio obtained from a combined modulated mechanical ($s = 20\%$) and steadily increasing thermal loading compared to Poisson's ratio of quartz [5]

In Fig. 7 the normalized evolution of Young's modulus for concrete subjected to different load levels ($s = 10$, 20, 30, 40%) is presented. For $s = 10\%$ the largest decrease in stiffness with increasing temperature is observed. For $s \geq 20\%$, this reduction of stiffness due to temperature loading is smaller. This difference is explained by the development of microcracks, resulting from strain incompatibilities of aggregates and cement paste. In case of loaded concrete $s \geq 20\%$ these microcracks are strongly reduced in comparison to unloaded concrete.

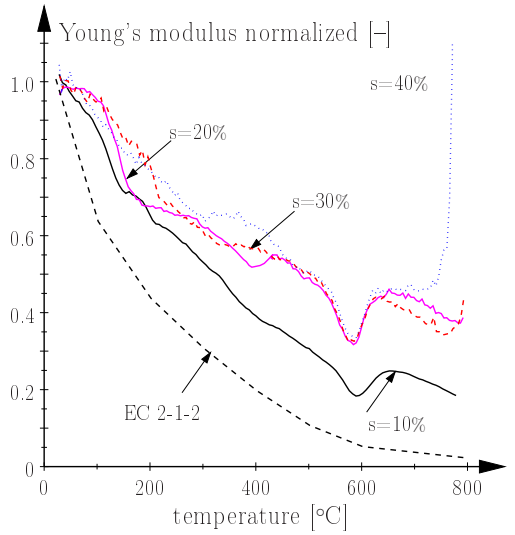

Figure 7: Normalized Young's modulus for different load levels ($s = 10$, 20, 30, 40%)

The influence of the load levels ($s = 10$, 20, 40%) on the evolution of Poisson's ratio is presented in Fig. 8. Since the measurement accuracy in radial direction (small deformations), produces a certain variation in the results, the lines are not smooth. Therefore, a sufficient interpretation of the obtained results before the temperature of quartz inversion can not be found easily, at higher temperatures, above 573 °C , it is observed, that for higher load levels the Poisson's ratio seems to increase (also beyond 0.5), this is due to increasing degradation of the concrete with leads in combination with high loading to large radial deformations (effects out of elastic range).

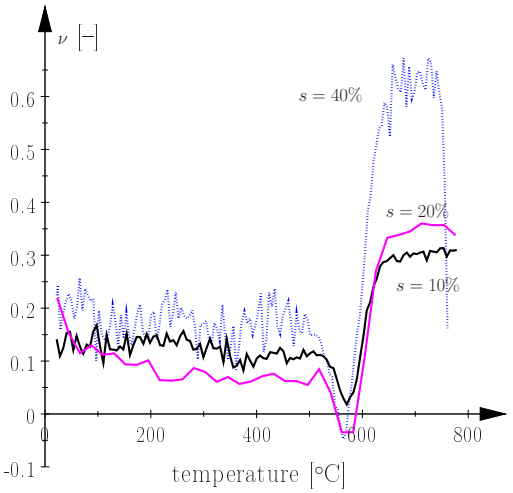

Figure 8: Compare of Poisson's ratio for different load levels ($s = 10$, 20, 30, 40%)

The evolution of shear and bulk modulus is displayed in Fig. 9 for different loaded concretes ($s = 10$, 40%). It can be observed that the shear modulus, almost linearly decreases with increasing temperature. The quartz transition at 573 °C influences only the bulk modulus.

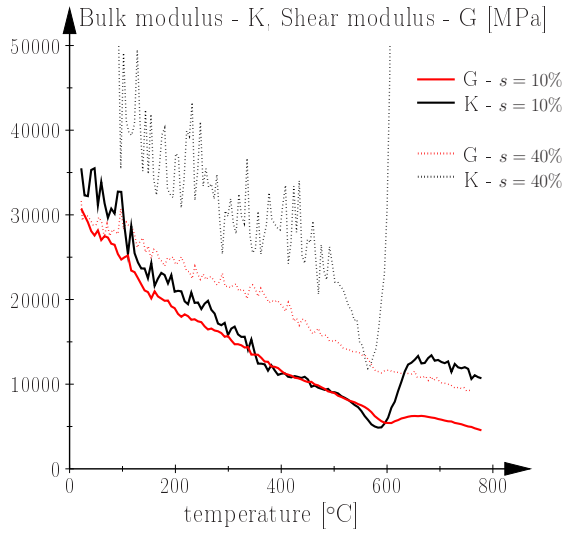

Figure 9: Evolution of shear modulus - G and bulk modulus - K for different load levels ($s = 10$, 40%)

3. Micromechanical model

In order to capture the strong influence of the aggregates on the overall concrete behavior a 2-phase material consisting of aggregates and cement paste is proposed in a first step. Hereby, the elastic properties of heated concrete are determined within the framework of continuum micromechanics (Mori Tanaka [6]).

The effective elastic properties of concrete, i.e., shear modulus G [MPa] and bulk modulus K [MPa] are given by:

$$G_{eff} = \frac{\sum_r f_r G_r [1 + \beta(\frac{G_r}{G_m} - 1)]^{-1}}{\Sigma f_r [1 + \beta(\frac{G_r}{G_m} - 1)]^{-1}}, \quad (3)$$

and

$$K_{eff} = \frac{\sum_r f_r K_r [1 + \alpha(\frac{K_r}{K_m} - 1)]^{-1}}{\Sigma f_r [1 + \alpha(\frac{K_r}{K_m} - 1)]^{-1}}, \quad (4)$$

with $r \in \{\text{matrix (cement paste), inclusions (aggregates)}\}$.

The coefficients α and β are calculated to:

$$\alpha = \frac{3K_m}{3K_m + 4G_m}, \quad (5)$$

and

$$\beta = \frac{6(K_m + 2G_m)}{5(3K_m + 4G_m)}. \quad (6)$$

In Equs. (3) to (6), index m stands for matrix. α and β represent the volumetric and deviatoric part of the Eshelby Tensor S, specialized for spherical inclusions.

Under the assumption that concrete only consists of 2-phases (aggregates and cement paste), the respective volume fraction is set to: $f_a/f_m = 0.75/0.25$. Since the aggregates consists of 89% siliceous material for the sake of simplicity it is assumed that that all aggregate is siliceous material. The mechanical properties are taken from the Literature (see Ref. [5]). In this paper the author tested the elastic properties of quartz up to 1100 °C with ultrasonic. The required bulk and shear moduli for different temperatures are presented in Tab. 1. In column 4 the Young's modulus of cement paste is displayed. In literature several author tested cement paste regarding the elastic properties at elevated temperatures (see Ref. [2, 7]). Unless the Young's modulus of cement paste under elevated temperatures is well researched, literature data for the corresponding Poisson's ratio is missing. Therefore for this first approach the Poisson's ratio is set equal to 0.24 for the whole temperature range.

Temp °C	K_a GPa	G_a GPa	E_c GPa	ν^* [–]
20	37.9	44.9	25	0.24
100	37.2	44.7	20.8	0.24
200	35.7	44.5	15.8	0.24
300	34.1	44.3	10.5	0.24
400	32.0	43.7	7.8	0.24
450	28.2	43.4	7.3	0.24
500	25.5	43.0	6.2	0.24
550	18.6	42.4	5.0	0.24
573	11.9	41.6	4.9	0.24
600	54.6	41.5	4.5	0.24
650	63.8	41.6	3.9	0.24
700	67.8	41.8	3.2	0.24

Table 1: Material parameters for aggregates and cement paste (* no literature for Poisson's ratio at high temperatures)

To calculate the bulk and shear modulus from cement paste out of Young's modulus and Poisson's ratio following formulas are used:

$$K = \frac{E}{3(1 - 2\nu)}, \quad (7)$$

and

$$G = \frac{E}{2(1 + \nu)}. \quad (8)$$

Using Equs. (7) and (8) for cement paste and evaluating Equs. (3) and (4) leads to following results:

Temp °C	K_{eff} GPa	G_{eff} GPa	ν_{eff} [–]	E_{eff} GPa
20	29.9	28.4	0.14	64.7
100	27.8	26.2	0.14	59.7
200	24.4	22.9	0.14	52.3
300	20.0	18.1	0.15	41.7
400	16.7	14.9	0.15	34.5
450	15.2	14.2	0.14	32.5
500	13.3	12.7	0.14	28.8
550	10.2	10.8	0.11	23.9
573	7.9	10.6	0.04	21.9
600	14.2	9.9	0.22	24.1
650	13.1	8.9	0.22	21.7
700	11.3	7.6	0.23	18.5

Table 2: Effective elastic properties for the 2-phase material

The results displayed in Tab. 2 are printing and compared to an experimental result ($s = 20\%$) in Fig. 10. The almost linear decrease of shear modulus like first presented in Fig. 9 is also observed in the 2-phase modeling.

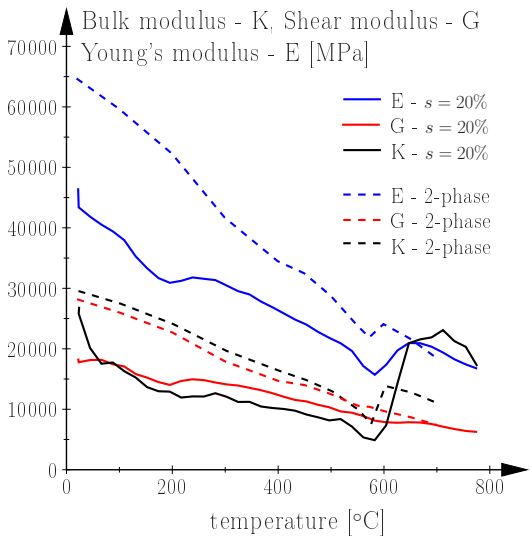

Figure 10: 2-phase (aggregates, cement paste; $f_a = 0.75$, $f_m = 0.25$) model results compared to experimentally observed results ($s = 20\%$)

Generally, the simulated Young's modulus appears to be to high, therefore in a next step, the micromechanical 2-phase model is extended to a more realistic 3-phase model to consider the pore space of concrete. The respective volume fraction of the proposed 3-phase model (aggregates, cement paste and air) is set to:

$f_a/f_m/f_p = 0.75/0.10/0.15$. Where, the bulk and shear modulus of air are set to 0. Applying of Equs. (3) and (4) leads to the new effective elastic properties presented in Tab. 3:

Temp °C	K_{eff} GPa	G_{eff} GPa	ν_{eff} [–]	E_{eff} GPa
20	20.9	20.1	0.14	45.6
100	19.2	18.2	0.14	41.5
200	16.5	15.6	0.14	35.5
300	13.0	12.0	0.15	27.5
400	10.7	9.6	0.15	22.2
450	9.7	9.1	0.14	20.9
500	8.5	8.0	0.14	18.3
550	6.6	6.8	0.12	15.1
573	5.3	6.6	0.06	14.0
600	8.2	6.2	0.20	14.8
650	7.5	5.5	0.20	13.2
700	6.3	4.6	0.21	11.2

Table 3: Effective elastic properties for the 3-phase material

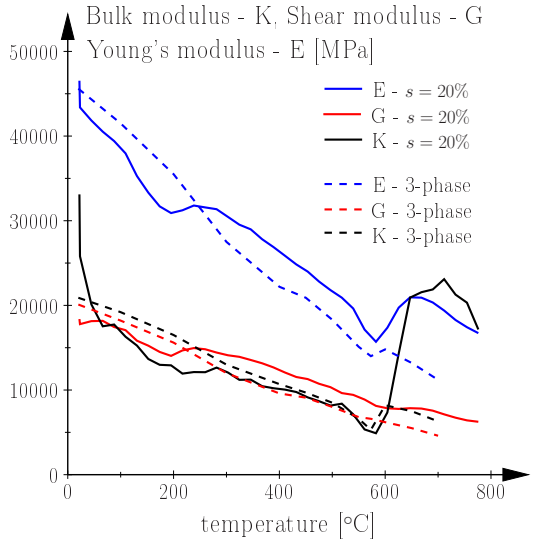

Figure 11: 3-phase (aggregates, cement paste, air; $f_a = 0.75$, $f_m = 0.10$, $f_p = 0.15$) model results compared to experimentally observed results ($s = 20\%$)

The results in Tab. 3 fit better to the experiments (see Fig. 11). The evolution can still not represent the real measured concrete behavior. This has 2 reasons: First the unknown material behavior of cement paste concerning the Poisson's ratio and second the change of volume fraction (damage of cement paste) due to heat up of concrete. Since, no data for our model in literature was found additional tests on cement paste are planned. Regarding the heavily damage of cement paste during heating up of concrete (dehydration, strain incompatibilities between aggregates and cement paste) the 3-phase model can be modified in a way, that the respective volume fractions for cement paste and air are not constant during the whole heating treatment. Meaning, for higher temperature levels the volume fraction for cement paste is reduced, and the volume fraction for air is increased by these latter reduction.

Finally, a comparison of Poisson's ratio evolution with increasing temperature is presented in Fig. 12, where the experiment is compared to the 2-phase and 3-phase model. The model can capture the quartz transition at 573 °C . For further improvement, additional cement paste tests are required.

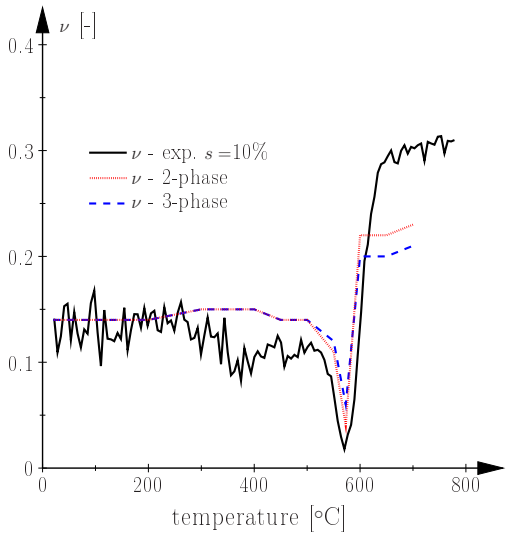

Figure 12: 3-phase (aggregates, cement paste, air; $f_a = 0.75$, $f_m = 0.10$, $f_p = 0.15$) model results compared to experimentally observed results ($s = 20\%$)

4. Conclusions

The conducted experiments showed that, the strain incompatibilities of cement paste and aggregates are strongly influencing the elastic properties of concrete up to a load level of $s = 20\%$. When concrete is higher loaded during heating up, the influence of these incompatibilities is not increasing, because the arising microcracks are closed by the high preloading. The finally proposed 3-phase model, can be used for simulating the elastic properties of concrete under high temperature subjected to combined mechanical and thermal loading.

5. Acknowledgments

This research was conducted with financial support by the Austrian Ministry for Transport, Innovation and Technology (bm.vit) within the KIRAS-project (Austrian security research program) 813794 "Sicherheit von Hohlraumbauten unter Feuerlast" ("Safety of underground structures under fire loading").

References

[1] Y. Anderberg and S. Thelandersson. Stress and deformation characteristics of concrete at high temperatures: 2. experimental investigation and material behaviour model. Technical Report 54, Lund Institute of Technology, Lund, 1976.

[2] W.P.S. Dias, G. A. Khoury, and P. J. E. Sullivan. Mechanical properties of hardened cement paste exposed to temperatures up to 700 c. *ACI Materials Journal*, 87(2):160–166, 1990.

[3] EN1992-1-2. *Eurocode 2 – Bemessung und Konstruktion von Stahlbeton- und Spannbetontragwerken – Teil 1-2: Allgemeine Regeln – Tragwerksbemessung für den Brandfall [Eurocode 2 – Design of concrete structures – Part 1-2: General rules – Structural fire design]*. European Commit-

tee for Standardization (CEN), 2007. In German.

[4] A. Galek, H. Moser, T. Ring, M. Zeiml, J. Eberhardsteiner, and R. Lackner. Mechanical and transport properties of concrete at high temperatures. In *Applied Mechanics and Materials*, volume 24-25, pages 1–11. Trans Tech Publications, Switzerland, 2010.

[5] D. L. Lakshtanov, Sinogeikin S. V., and Bass J.D. High-temperature phase transitions and elasticity of silica polymorphs. *Physics and Chemistry of Minerals*, 34(1):11–22, 2007.

[6] T. Mori and K. Tanaka. Average stress in martix and average elastic energy of materials with misfitting inclusions. *Acta Metallurgica*, 21:571–574, 1973.

[7] J.B. Odelson, E. A. Kerr, and W. Vichit-Vadakan. Young's modulus of cement paste at elevated temperatures. *Cement and Concrete Research*, 37:258–263, 2007.

[8] L. T. Phan and N. J. Carino. Review of mechanical properties of HSC at elevated temperatures. *Journal of Materials in Civil Engineering*, 10(1):58–64, 1998.

[9] U. Schneider. Concrete at high temperature – a general review. *Fire Safety Journal*, 13:55–68, 1988.

[10] M. J. Terro. Numerical modeling of the behavior of concrete structures in fire. *ACI Structural Journal*, 95(2):183–193, 1998.